

## Research Article

# Effect of Internal Heat Source on the Onset of Double-Diffusive Convection in a Rotating Nanofluid Layer with Feedback Control Strategy

I. K. Khalid,<sup>1</sup> N. F. M. Mokhtar,<sup>1,2</sup> I. Hashim,<sup>3</sup> Z. B. Ibrahim,<sup>2</sup> and S. S. A. Gani<sup>4</sup>

<sup>1</sup>*Institute for Mathematical Research, Universiti Putra Malaysia, 43400 Serdang, Selangor, Malaysia*

<sup>2</sup>*Department of Mathematics, Faculty of Science, Universiti Putra Malaysia, 43400 Serdang, Selangor, Malaysia*

<sup>3</sup>*School of Mathematical Sciences, Faculty of Science and Technology, National University of Malaysia, 43600 Bangi, Selangor, Malaysia*

<sup>4</sup>*Department of Chemistry, Faculty of Science, Universiti Putra Malaysia, 43400 Serdang, Selangor, Malaysia*

Correspondence should be addressed to N. F. M. Mokhtar; [norfadzillah.mokhtar@gmail.com](mailto:norfadzillah.mokhtar@gmail.com)

Received 15 February 2017; Revised 1 May 2017; Accepted 5 June 2017; Published 13 July 2017

Academic Editor: Xavier Leoncini

Copyright © 2017 I. K. Khalid et al. This is an open access article distributed under the Creative Commons Attribution License, which permits unrestricted use, distribution, and reproduction in any medium, provided the original work is properly cited.

A linear stability analysis has been carried out to examine the effect of internal heat source on the onset of Rayleigh–Bénard convection in a rotating nanofluid layer with double diffusive coefficients, namely, Soret and Dufour, in the presence of feedback control. The system is heated from below and the model used for the nanofluid layer incorporates the effects of thermophoresis and Brownian motion. Three types of bounding systems of the model have been considered which are as follows: both the lower and upper bounding surfaces are free, the lower is rigid and the upper is free, and both of them are rigid. The eigenvalue equations of the perturbed state were obtained from a normal mode analysis and solved using the Galerkin method. It is found that the effect of internal heat source and Soret parameter destabilizes the nanofluid layer system while increasing the Coriolis force, feedback control, and Dufour parameter helps to postpone the onset of convection. Elevating the modified density ratio hastens the instability in the system and there is no significant effect of modified particle density in a nanofluid system.

## 1. Introduction

The importance of understanding convective heat transfer in nanofluids has been a topic of interest for the last few years. A nanofluid, that is, a colloidal mixture of nanosized particles (1–100 nm), and a base fluid (nanoparticle fluid suspension) was first introduced by Choi [1]. Nanofluids possess their stability due to the small size of their particles, low weight, and less chance of sedimentation. Subsequently, there have been tremendous attempts to observe the enhancement of thermal conductivity in a nanofluid. The earliest investigation was reported by Masuda et al. [2], followed by Xuan and Li [3], Eastman et al. [4], and Das et al. [5]. Buongiorno [6] discussed the seven slip mechanisms that can produce a relative velocity between the nanoparticles and the base fluid. These are inertia, Brownian diffusion, thermophoresis, diffusiophoresis, Magnus effect, fluid drainage, and gravity settling. He concluded that the effects of Brownian diffusion

and thermophoresis are important for convective transport in nanofluids and his model is the basis for the present study. Tzou [7, 8] employed Buongiorno's model to investigate the thermal instability problem and found that nanofluids are less stable than regular fluids. Alloui et al. [9] studied the natural convection of nanofluids in a shallow cavity heated from below. Nield and Kuznetsov [10] studied the parameters involved in the onset of convection in a horizontal nanofluid layer of finite depth. A linear analysis of the Rayleigh–Bénard instability for a nanofluid is performed by Yadav et al. [11]. Haddad et al. [12] reported that the thermophoresis and Brownian motion are significant in the thermal enhancement of the natural convection in a nanofluid layer. Recently, Gupta et al. [13] investigated the thermosolutal convection in a horizontal nanofluid layer heated from below.

Soret diffusion, or also known as thermal diffusion, and Dufour diffusion, also known as thermodiffusion [14], are

important in both Newtonian and non-Newtonian convective heat and mass transfer, and they are often encountered in chemical process engineering and in high-speed aerodynamics. Such effects are significant for gases of intermediate molecular weight in the coupled heat and mass transfer in binary systems. Hurlle and Jakeman [15] demonstrated the Soret-driven thermosolutal convection both theoretically and experimentally using a water-methanol mixture. Then, Platten and Chavepeyer [16] continued using a water-ethanol mixture while Caldwell [17] extended the investigation using a salt solution. The linear stability of experimental Soret convection in a water-ethanol mixture under various boundary conditions had been investigated by Knobloch and Moore [18] with an emphasis on the Biot number. The thermocapillary instability in a binary fluid on the onset of convection with Soret effect and other physical influences also had been studied [19–21]. Later, Nield and Kuznetsov [22] extended [10] and used the linear instability theory to study the onset of double-diffusive convection in a horizontal layer of a nanofluid. Kuznetsov and Nield [23], Yadav et al. [24, 25], and Agarwal et al. [26] investigated double-diffusive convection in a porous medium permeated by a nanofluid layer. The authors in [27–29] added other effects to the system of double-diffusive convection in a nanofluid layer.

The thermal instability induced by uniform internal heat generation arising in a horizontal fluid layer has attracted the attention of many researchers [30–38]. It is found that an internal heat source decreases the stability of the fluid layer. Yadav et al. [39, 40] and Nield and Kuznetsov [41] included the effect of an internal heat source on the thermal instability in a nanofluid layer and found that the heat source advances the onset of convection. Recently, Wakif et al. [42] studied the combined effects of rotation and internal heating on a radiating nanofluid layer using the power series method (PSM) solely at both the upper and lower rigid boundaries.

The Coriolis force which is due to rotation in a system has an important effect on convective instability. Chandrasekhar [43] discussed Rayleigh–Bénard convection in a regular fluid with a linear temperature profile, both with and without the effect of rotation. In 1966, Vidal and Acrivos [44] included the effect of Coriolis force on the thermocapillary type of convection. Later, McConaghy and Finlayson [45], Takashima and Namikawa [46], Friedrich and Rudraiah [47], and Douiebe et al. [48] extended the previous analysis with other aspects of the problem. Meanwhile, several authors [49–52] have investigated the convective instability in a rotating fluid layer induced by buoyancy and thermocapillary, which has received profound attention from the engineering industry. Yadav et al. [53–56] studied the effect of rotation in a nanofluid layer and found that an increase in the Taylor number delays the onset of convection.

The use of feedback control in stabilizing the thermal convection was by Wang et al. [57] and they managed to inhibit the chaotic behaviour in the fluid layer by applying proportional control in a thermal convection loop. Later, Tang [58] and Tang and Bau [59, 60] showed that, with the use of a feedback controller, the critical Rayleigh number for the onset of convection can be significantly increased. Tang and Bau [61–64] and Howle [65–67] demonstrated

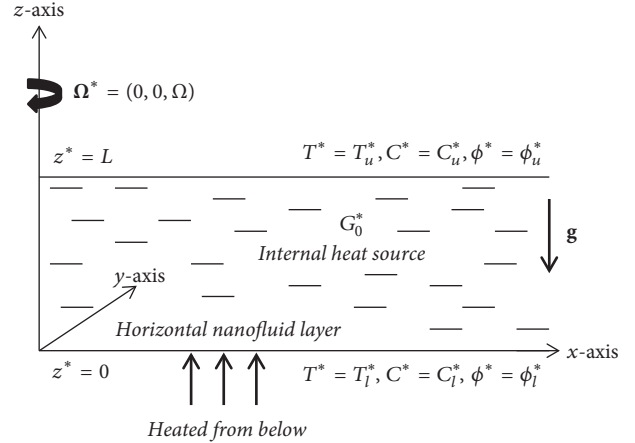


FIGURE 1: Physical configuration and coordinate system.

experimentally that feedback control can be used to stable the system through the use of the control strategy. It is interesting to note that similar control strategies can be used to modify the flow patterns of shear flows [68] and surface-tension driven flows [69]. Further, many researchers have attempted to include other effects with the feedback control [70–75] on convection due to buoyancy and surface-tension.

In this paper, we intend to scrutinize the effect of internal heat source on the thermal instability of double-diffusive convection in a rotating nanofluid layer with feedback control. As in industrial heat transfer, heat needs to be efficiently controlled whether being added, removed, or transferred from one process stream to another. It is reported that between 20% and 50% of industrial energy input is lost as waste heat [76], which has attracted numerous studies on energy efficiency, recovering waste heat, and so on. This motivated us to contribute mathematically by providing a mathematical model that can simulate the influence of an internal heat source and feedback control in a nanofluid layer with other crucial parameters. We assume the nanofluid layer is heated from below and the lower-upper boundary conditions are considered to be free-free, rigid-free, and rigid-rigid. For systems that have thermal gradient and energy flux due to a mass concentration, Soret and Dufour coefficients are vital. To understand deeply the reaction of these two coefficients in a rotating nanofluid layer with internal heat source and feedback controller, we considered the interdiffusion parameter in the system. A linear stability analysis is performed, and the eigenvalue is obtained by employing the Galerkin technique. Numerical computations of the various relevant parameters are presented graphically.

## 2. Mathematical Formulation

Cartesian coordinates  $(x, y, z)$  are used, where the  $z$ -axis points vertically upward. From now on, we denote the dimensional (nondimensional) variables with (without) asterisks. Consider a horizontal layer of a rotating incompressible nanofluid of thickness  $L$  confined between the planes  $z^* \in [0, L]$  and subjected to a uniform internal heat source  $G_0^*$  is heated from below as shown in Figure 1. The nanofluid layer

rotates about the vertical axis at a constant angular velocity,  $\mathbf{\Omega}^* = (0, 0, \Omega)$ . The stability of a horizontal rotating nanofluid layer in the presence of internal heat source is examined. The temperature, solute concentration, and nanoparticle volume fraction at the lower and upper walls are denoted by  $T_l^*$ ,  $C_l^*$ , and  $\phi_l^*$  at  $z = 0$  and  $T_u^*$ ,  $C_u^*$ , and  $\phi_u^*$  at  $z = L$ , respectively. Following Nield and Kuznetsov [22], the governing equations that describe the Boussinesq flow under this model with the presence of the effect of rotation and internal heat source are

$$\begin{aligned} \nabla^* \cdot \mathbf{U}^* &= 0, \\ \rho_l \left[ \frac{\partial \mathbf{U}^*}{\partial t^*} + (\mathbf{U}^* \cdot \nabla^*) \mathbf{U}^* \right] &= -\nabla^* p^* + \mu \nabla^{*2} \mathbf{U}^* \\ &+ (2\rho_l \mathbf{U}^* \times \mathbf{\Omega}^*) + \mathbf{g} \left[ \phi^* \rho_p \right. \\ &\left. + (1 - \phi^*) \rho_l [1 - \alpha_T (T^* - T_l^*) - \alpha_C (C^* - C_l^*)] \right], \\ \rho c \left[ \frac{\partial T^*}{\partial t^*} + (\mathbf{U}^* \cdot \nabla^*) T^* \right] &= \kappa \nabla^{*2} T^* + G_0^* \\ &+ \rho c [D_{TC} \nabla^{*2} C^*] + \rho_p c_p \left[ D_B \nabla^* \phi^* \cdot \nabla^* T^* \right. \\ &\left. + \left( \frac{D_T}{T_u^*} \right) \nabla^* T^* \cdot \nabla^* T^* \right], \\ \left[ \frac{\partial C^*}{\partial t^*} + (\mathbf{U}^* \cdot \nabla^*) C^* \right] &= D_S \nabla^{*2} C^* + D_{CT} \nabla^{*2} T^*, \\ \left[ \frac{\partial \phi^*}{\partial t^*} + (\mathbf{U}^* \cdot \nabla^*) \phi^* \right] &= D_B \nabla^{*2} \phi^* + \frac{D_T}{T_u^*} \nabla^{*2} T^*, \end{aligned} \quad (1)$$

where  $\mathbf{U}^* = (u, v, w)$  is the velocity,  $\rho$  is the density,  $\rho_l$  is the nanofluid density at the reference temperature  $T_l^*$ ,  $\rho_p$  is the nanoparticle mass density,  $t^*$  is time,  $p^*$  is the pressure,  $\mu$  is the viscosity,  $\mathbf{g}$  is the gravitational force,  $\phi^*$  is the nanoparticle volume fraction,  $G_0^*$  is the uniform internal heat source,  $\alpha_T$  is the thermal volumetric coefficient,  $T^*$  is the temperature,  $\alpha_C$  is the solutal volumetric coefficient,  $C^*$  is the solute concentration,  $c$  is the specific heat,  $c_p$  is the specific heat of the nanoparticles,  $\kappa$  is the nanofluid's thermal conductivity,  $D_{TC}$  is the Dufour diffusivity,  $D_B$  is the Brownian diffusion coefficient,  $D_T$  is the thermophoretic diffusion coefficient,  $D_S$  is the solutal diffusivity, and  $D_{CT}$  is the Soret diffusivity.

In the steady state, the upper surface of the nanofluid layer is flat and stationary. Following Char and Chiang [31], the pressure and temperature fields are

$$\begin{aligned} p^*(z) &= p_l^* - \rho_l \left[ 1 + \frac{\alpha z^* \Delta T^*}{2L} - \frac{\alpha L \Delta T^*}{2L} \right] \mathbf{g}(z^* - L), \\ T^*(z) &= T_l^* - \frac{G_0^*}{2\kappa} z^{*2} + \frac{G_0^* L}{2\kappa} z^* - \frac{\Delta T^*}{L} z^*, \end{aligned} \quad (2)$$

where  $p_l^*$  is the reference pressure and  $\Delta T^*$  is the temperature difference across the fluid layer. Then, (1) are nondimensionalised using the following definitions:

$$\begin{aligned} (x, y, z) &= \frac{x^*, y^*, z^*}{L}, \\ p &= L^2 \frac{p^*}{\mu \alpha_f}, \\ t &= \alpha_f \frac{t^*}{L^2}, \\ \psi &= L^2 \frac{\psi^*}{\alpha_f}, \\ \phi &= \frac{\phi^* - \phi_l^*}{\phi_u^* - \phi_l^*}, \\ (u, v, w) &= L \frac{u^*, v^*, w^*}{\alpha_f}, \\ T &= \frac{T^* - T_l^*}{\Delta T^*}, \\ C &= \frac{C^* - C_l^*}{\Delta C^*}, \end{aligned} \quad (3)$$

where  $\alpha_f = \kappa/\rho c$  is the thermal diffusivity and  $\psi$  is the vorticity due to rotation in the  $z$  component.

By substituting (3) into (1), the following nondimensional variables are obtained:

$$\begin{aligned} \nabla \cdot \mathbf{U} &= 0, \\ \frac{1}{\text{Pr}} \left[ \frac{\partial \mathbf{U}}{\partial t} + \mathbf{U} \cdot \nabla \mathbf{U} \right] &= -\nabla p + \nabla^2 \mathbf{U} - \text{Rm} \hat{\mathbf{e}}_z + \text{Ra} T \hat{\mathbf{e}}_z \\ &+ \frac{\text{Rs}}{\text{Le}} C \hat{\mathbf{e}}_z - \text{Rn} \phi \hat{\mathbf{e}}_z \\ &+ \sqrt{\text{Ta}} (\mathbf{U} \times \hat{\mathbf{e}}_z), \\ \left[ \frac{\partial T}{\partial t} + \mathbf{U} \cdot \nabla T \right] &= \nabla^2 T + \frac{N_B}{\text{Ln}} \nabla \phi \cdot \nabla T + \frac{N_A N_B}{\text{Ln}} \nabla T \\ &\cdot \nabla T + \text{Df} \nabla^2 C \\ &+ [Q(1 - 2z) - 1] w, \\ \left[ \frac{\partial C}{\partial t} + \mathbf{U} \cdot \nabla C \right] &= \frac{1}{\text{Le}} \nabla^2 C + \text{Sr} \nabla^2 T, \\ \left[ \frac{\partial \phi}{\partial t} + \mathbf{U} \cdot \nabla \phi \right] &= \frac{1}{\text{Ln}} \nabla^2 \phi + \frac{N_A}{\text{Ln}} \nabla^2 T, \end{aligned} \quad (4)$$

where  $\hat{\mathbf{e}}_z = (0, 0, 1)$  is the unit vector in the  $z$  direction,  $\text{Pr} = \mu/\rho \alpha_f$  is the Prandtl number,  $\text{Rm} = [\rho_p \phi_l^* + \rho(1 - \phi_l^*)] g L^3 / \mu \alpha_f$  is the basic-density Rayleigh number,  $\text{Ra} = \rho g \alpha_T L^3 \Delta T^* / \mu \alpha_f$  is the thermal Rayleigh number,  $\text{Rs} = \rho g \alpha_C L^3 \Delta C^* / \mu D_s$  is the solutal Rayleigh number,  $\text{Le} = \alpha_f / D_s$  is the Lewis number,  $\text{Rn} = (\rho_p - \rho)(\phi_u^* - \phi_l^*) g L^3 / \mu \alpha_f$

is the nanoparticle concentration Rayleigh number,  $Ta = (4\Omega^{*2}/\mu^2)L^4$  is the Taylor number,  $N_B = ((\rho c)_p/(\rho c)_f)(\phi_u^* - \phi_l^*)$  is the modified particle-density increment,  $Ln = \alpha_f/D_B$  is the nanofluid Lewis number,  $N_A = D_T\Delta T^*/D_B T_u^*(\phi_u^* - \phi_l^*)$  is the modified density ratio,  $Df = D_{TC}\Delta C^*/\alpha_f\Delta T^*$  is the Dufour parameter,  $Sr = D_{CT}\Delta T^*/\alpha_f\Delta C^*$  is the Soret parameter, and  $Q = G_0^*L^2/2\kappa\Delta T^*$  represents the internal heat generation.

We seek a time-independent quiescent solution for (4) with the temperature, concentration, and nanoparticle volume fraction varying only in the  $z$  direction, that is, a basic state solution of the form

$$\begin{aligned}(u, v, w) &= (0, 0, 0), \\ p &= p_b(z), \\ T &= T_b(z), \\ C &= C_b(z), \\ \phi &= \phi_b(z).\end{aligned}\quad (5)$$

Suppose that the basic state is disturbed by an infinitesimal thermal perturbation. We now superimpose perturbations on the basic solution. We write

$$\begin{aligned}(u, v, w, p, T, C, \phi, \psi) \\ = [0, 0, 0, p_b(z), T_b(z), C_b(z), \phi_b(z), \psi_b(z)] \\ + [u', v', w', p', T', C', \phi', \psi'].\end{aligned}\quad (6)$$

We substitute (6) into (4) and linearise them by neglecting the products of primed quantities and obtain

$$\nabla \cdot \mathbf{U}' = 0, \quad (7)$$

$$\begin{aligned}\frac{1}{Pr} \frac{\partial \mathbf{U}'}{\partial t} \\ = -\nabla p' + \nabla^2 \mathbf{U}' + Ra T' \hat{\mathbf{e}}_z + \frac{Rs}{Le} C' \hat{\mathbf{e}}_z - Rn \phi' \hat{\mathbf{e}}_z \\ + \sqrt{Ta} (\mathbf{U}' \times \hat{\mathbf{e}}_z),\end{aligned}\quad (8)$$

$$\begin{aligned}\frac{\partial T'}{\partial t} - [Q(1-2z) - 1] w' \\ = \nabla^2 T' + \frac{N_B}{Ln} \left[ \frac{\partial T'}{\partial z} - \frac{\partial \phi'}{\partial z} \right] - \frac{2N_A N_B}{Ln} \frac{\partial T'}{\partial z} \\ + Df \nabla^2 C',\end{aligned}\quad (9)$$

$$\left[ \frac{\partial C'}{\partial t} - w' \right] = \frac{1}{Le} \nabla^2 C' + Sr \nabla^2 T', \quad (10)$$

$$\left[ \frac{\partial \phi'}{\partial t} + w' \right] = \frac{1}{Ln} \nabla^2 \phi' + \frac{N_A}{Ln} \nabla^2 T'. \quad (11)$$

The parameter  $Rm$  is not included in these and subsequent equations. It is just a measure of the basic static pressure gradient.

Operating curl twice to (8) and using the curl identity together with (7), we obtain

$$\begin{aligned}\left[ \nabla^4 - \frac{1}{Pr} \frac{\partial}{\partial t} \nabla^2 \right] w' + \frac{Rs}{Le} \nabla_P^2 C' - Rn \nabla_P^2 \phi' + Ra \nabla_P^2 T' \\ - \sqrt{Ta} \frac{\partial \Psi'}{\partial z} = 0,\end{aligned}\quad (12)$$

$$\left[ \nabla^2 - \frac{1}{Pr} \frac{\partial}{\partial t} \right] \Psi' + \sqrt{Ta} \frac{\partial w'}{\partial z} = 0,$$

where  $\nabla_P^2$  is the horizontal two-dimensional Laplacian operator.

The proposed normal mode representation is

$$\begin{aligned}(w', T', C', \phi', \psi') \\ = [W(z), \Theta(z), \eta(z), \phi(z), \Psi(z)] e^{[i(a_x x + a_y y) + \sigma t]},\end{aligned}\quad (13)$$

where  $(a_x, a_y)$  is the wavevector in the  $(x, y)$  plane,  $a^2 = a_x^2 + a_y^2$  is the square of the wavenumber, and  $\sigma$  is the growth parameter.

Substituting (13) into (9)–(12) and neglecting the terms of the second and higher orders in the perturbations, we obtain

$$\begin{aligned}(D^2 - a^2)^2 W - a^2 Ra \Theta - a^2 \frac{Rs}{Le} \eta + a^2 Rn \phi \\ - \sqrt{Ta} D \Psi = 0, \\ [1 - Q(1 - 2z)] W \\ + \left[ D^2 - a^2 + \frac{N_B}{Ln} D - 2 \frac{N_A N_B}{Ln} D \right] \Theta - \frac{N_B}{Ln} D \phi \\ + Df (D^2 - a^2) \eta = 0, \\ W + Sr (D^2 - a^2) \Theta + \frac{1}{Le} (D^2 - a^2) \eta = 0, \\ W - \frac{N_A}{Ln} (D^2 - a^2) \Theta - \frac{1}{Ln} (D^2 - a^2) \phi = 0, \\ \sqrt{Ta} DW + (D^2 - a^2) \Psi = 0,\end{aligned}\quad (14)$$

where  $a = \sqrt{a_x^2 + a_y^2}$  is the wavenumber and  $D = d/dz$ .

Following the proportional feedback control [69], the continuously distributed actuators and sensors are arranged in a way that, for every sensor, there is an actuator positioned directly beneath it. The determination of a control  $q(t)$  can be accomplished using the proportional-integral-differential (PID) controller of the form

$$q(t) = r + K [e(t)], \quad (15)$$

where  $r$  is the calibration of the control,  $e(t) = \widehat{m}(t) + m(t)$  is an error or deviation from the measurement,  $\widehat{m}(t)$ , from some desired reference value,  $m(t)$ ,  $K$  is the scalar controller gain where  $K = K_P + K_D(d/dt) + K_I \int_0^t dt$ ,  $K_P$  is the proportional gain,  $K_D$  is the differential gain, and  $K_I$  is the integral gain.

Based on (15), for one sensor plane and proportional feedback control, the actuator modifies the heated surface temperature using a proportional relation between the upper,  $z = 1$ , and the lower,  $z = 0$ , thermal boundaries for the perturbation field

$$T'(x, y, 0, t) = -KT'(x, y, 1, t), \quad (16)$$

where  $T'$  denotes the deviation of the temperature of fluid from its conductive state.

Equations (14) are solved subject to the appropriate boundary conditions. Considering the proportional controller,  $K$  positioned at the lower boundary of nanofluid layer, we will have

$$W = DW = \Theta(0) + K\Theta(1) = \phi = \eta = \Psi = D\Psi = 0 \quad (17)$$

at  $z = 0$ .

We assumed that the upper boundary is nondeformable and insulating to temperature perturbations. The suitable upper boundary conditions are as follows.

For the upper free boundary, which is at  $z = 1$ , we have

$$W = D^2W = D\Theta = \phi = \eta = D\Psi = 0 \quad \text{at } z = 1. \quad (18)$$

For the upper rigid boundary, which is at  $z = 1$ , we have

$$W = DW = D\Theta = \phi = \eta = D\Psi = 0 \quad \text{at } z = 1. \quad (19)$$

The Galerkin-type weighted residuals method is applied to find an approximate solution to the system. The variables are written in a series of basis functions:

$$\begin{aligned} W &= \sum_{i=1}^n A_i W_i, \\ \Theta &= \sum_{i=1}^n B_i \Theta_i, \\ \eta &= \sum_{i=1}^n C_i \eta_i, \\ \phi &= \sum_{i=1}^n D_i \phi_i, \\ \Psi &= \sum_{i=1}^n E_i \Psi_i, \end{aligned} \quad (20)$$

where  $A_i, B_i, C_i, D_i,$  and  $E_i$  are constants and the basis functions  $W_i, \Theta_i, \eta_i, \phi_i,$  and  $\Psi_i$  where  $i = 1, 2, 3, \dots$  will be chosen corresponding to the free-free, rigid-free, and rigid-rigid lower-upper boundary conditions:

$$W = \eta = \phi = \sin(z\pi),$$

$$\Theta = z(2 - z),$$

$$\Psi = z(3z - 2z^2),$$

$$W = z^2(1 - z)(3 - 2z),$$

$$\Theta = z(2 - z),$$

$$\eta = \phi = z(1 - z),$$

$$\Psi = z(3z - 2z^2),$$

$$W = z^2(1 - z)^2,$$

$$\Theta = z(2 - z),$$

$$\eta = \phi = z(1 - z),$$

$$\Psi = z(3z - 2z^2).$$

(21)

Substitute (20) into (14) and make the expressions on the left-hand sides of those equations (the residuals) orthogonal to the trial functions, thereby obtaining a system of  $5N$  linear algebraic equations in the  $5N$  unknowns. The vanishing of the determinant of the coefficients produces the eigenvalue equation for the system. One can regard  $Ra$  as the eigenvalue and thus  $Ra$  is found in terms of the other parameters.

Perform an integration by parts with respect to  $z$  between  $z \in [0, 1]$ . By using boundary conditions (21), we obtain the system of linear homogeneous algebraic equations

$$\begin{aligned} a_{ji}W_i + b_{ji}\Theta_i + c_{ji}\eta_i + d_{ji}\phi_i + e_{ji}\Psi_i &= 0, \\ f_{ji}W_i + g_{ji}\Theta_i + h_{ji}\eta_i + i_{ji}\phi_i + j_{ji}\Psi_i &= 0, \\ k_{ji}W_i + l_{ji}\Theta_i + m_{ji}\eta_i + n_{ji}\phi_i + o_{ji}\Psi_i &= 0, \\ p_{ji}W_i + q_{ji}\Theta_i + r_{ji}\eta_i + s_{ji}\phi_i + t_{ji}\Psi_i &= 0, \\ u_{ji}W_i + v_{ji}\Theta_i + w_{ji}\eta_i + x_{ji}\phi_i + y_{ji}\Psi_i &= 0. \end{aligned} \quad (22)$$

The above set of homogeneous algebraic equations can have a nontrivial solution if and only if

$$\begin{vmatrix} a_{ji} & b_{ji} & c_{ji} & d_{ji} & e_{ji} \\ f_{ji} & g_{ji} & h_{ji} & i_{ji} & j_{ji} \\ k_{ji} & l_{ji} & m_{ji} & n_{ji} & o_{ji} \\ p_{ji} & q_{ji} & r_{ji} & s_{ji} & t_{ji} \\ u_{ji} & v_{ji} & w_{ji} & x_{ji} & y_{ji} \end{vmatrix} = 0. \quad (23)$$

The eigenvalue has to be obtained from the characteristic (23).

The obtained eigenvalues of the Rayleigh number,  $Ra$ , for the lower-upper rigid-rigid boundary conditions are

$$Ra = \frac{42 \left[ (1/140) a^2 Rn \Lambda_v - \Lambda_w - (1/140 Le) a^2 Rs \Lambda_x + (3/70) \sqrt{Ta} \Lambda_y \right]}{a^2 \Lambda_z}, \quad (24)$$

where

$$\begin{aligned}
\Lambda_v &= \left( \lambda_6 \lambda_1 \lambda_2 \lambda_3 + \frac{1}{140} \lambda_4 \lambda_1 \lambda_3 + \frac{1}{140} \lambda_5 \lambda_2 \lambda_3 \right. \\
&\quad \left. - \frac{1}{140} \lambda_5 \lambda_7 \lambda_3 \right), \\
\Lambda_w &= \lambda_9 \left( \lambda_4 \lambda_1 \lambda_8 \lambda_3 - \lambda_5 \lambda_7 \lambda_8 \lambda_3 - \frac{1}{6} \frac{N_B \lambda_1 \lambda_2 \lambda_3}{\text{Ln}} \right), \\
\Lambda_x &= \left( \lambda_6 \lambda_7 \lambda_8 \lambda_3 - \frac{1}{140} \lambda_4 \lambda_8 \lambda_3 + \frac{1}{840} \frac{N_B \lambda_2 \lambda_3}{\text{Ln}} \right. \\
&\quad \left. - \frac{1}{840} \frac{N_B \lambda_7 \lambda_3}{\text{Ln}} \right), \\
\Lambda_y &= \left( -\frac{3}{70} \lambda_4 \lambda_1 \sqrt{\text{Ta}} \lambda_8 + \frac{3}{70} \lambda_5 \lambda_7 \sqrt{\text{Ta}} \lambda_8 \right. \\
&\quad \left. + \frac{1}{140} \frac{N_B \lambda_1 \sqrt{\text{Ta}} \lambda_2}{\text{Ln}} \right), \\
\Lambda_z &= \left( -\lambda_6 \lambda_1 \lambda_8 \lambda_3 - \frac{1}{140} \lambda_5 \lambda_8 \lambda_3 - \frac{1}{840} \frac{N_B \lambda_1 \lambda_3}{\text{Ln}} \right)
\end{aligned} \tag{25}$$

is defined as

$$\begin{aligned}
\lambda_1 &= \frac{3}{10} \frac{a^2}{\text{Le}} - \frac{1}{3} \frac{4+a^2}{\text{Le}} + \frac{1}{\text{Le}}, \\
\lambda_2 &= -\frac{11}{20} \frac{N_A a^2}{\text{Ln}} + \frac{1}{3} \frac{N_A (4+2a^2)}{\text{Ln}} - \frac{N_A}{\text{Ln}}, \\
\lambda_3 &= \frac{13}{35} a^2 + \frac{6}{5}, \\
\lambda_4 &= -\frac{8}{15} a^2 - \frac{4}{3} \frac{N_B}{\text{Ln}} - \frac{4}{3} - \frac{8}{3} \frac{N_B N_A}{\text{Ln}} - K, \\
\lambda_5 &= \frac{11}{20} \text{Df} a^2 - \frac{1}{3} \text{Df} (4+2a^2) + \text{Df}, \\
\lambda_6 &= \frac{1}{420} Q + \frac{1}{42}, \\
\lambda_7 &= \frac{11}{20} \text{Sr} a^2 - \frac{1}{3} \text{Sr} (4+2a^2) + \text{Sr}, \\
\lambda_8 &= -\frac{3}{10} \frac{a^2}{\text{Ln}} + \frac{1}{3} \frac{4+a^2}{\text{Ln}} - \frac{1}{\text{Ln}}, \\
\lambda_9 &= \frac{4}{5} + \frac{1}{630} a^4 + \frac{4}{105} a^2.
\end{aligned} \tag{26}$$

### 3. Results and Discussion

In this paper, the resulting eigenvalue problem in double-diffusive convection on a horizontal rotating nanofluid layer was solved analytically using Galerkin method. A linear stability analysis has been employed, and three types of lower-upper boundary conditions have been considered which are free-free, rigid-free, and rigid-rigid. The values of the various relevant parameters were chosen according to the range of

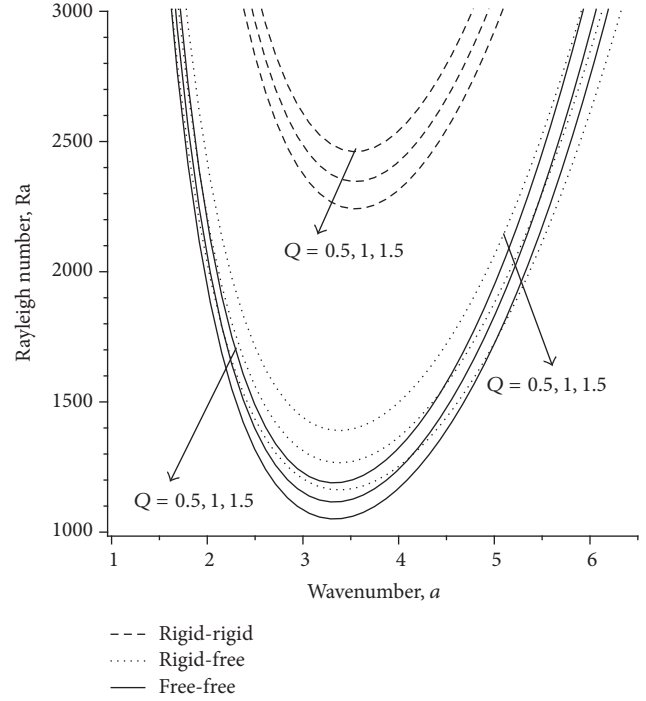


FIGURE 2: Impact of  $Q$  on  $Ra$  against  $a$ .

parameter values proposed by Chand and Rana [27]. The obtained results have been presented graphically to illustrate the impact of various parameters on the Rayleigh number  $Ra$  as well as critical Rayleigh number  $Ra_c$ .

Test computations have been performed and we compared our results with Chandrasekhar [43] and Yadav et al. [55] for the limiting case of nanofluid (regular fluids) in the absence of internal heat source, feedback control, Soret parameter, and Dufour parameter. The comparison results of critical Rayleigh number  $Ra_c$  for the rigid-rigid boundary conditions are presented in Table 1. As can be seen in the table, our results are in good agreement with those reported in [43, 55] and thus verify the accuracy of our analysis.

The influence of internal heat source,  $Q$ , on the onset of Rayleigh-Bénard convection in a nanofluid layer is illustrated in Figure 2. It can be seen clearly that an increase of  $Q$  decreases the Rayleigh number spontaneously. This indicates that the system becomes destabilized because of an increase in the energy supply to the system that leads to an increase in the rate of disturbances in the nanofluid layer. As for the type of boundaries, the curve that represents rigid-rigid boundaries dominates the upper part of the graph and this reveals that the onset of convection can be delayed using this type of boundary.

Figure 3 shows the Rayleigh number,  $Ra$ , versus the wavenumber  $a$  for different values of Taylor number,  $Ta$ , with various horizontal boundary conditions.  $Ra$  increases with increasing of the Taylor number  $Ta$ , indicating that the Coriolis force due to a rotation inhibits the onset of Rayleigh-Bénard convection in a nanofluid layer. The fluid moves to the horizontal plane with higher velocity because of

TABLE I: Comparison of  $Ra_c$  in rigid-rigid boundary conditions for the limiting case of nanofluid.

Ta	Chandrasekhar [43]	Yadav et al. [55]	Present study
	Rigid-rigid $Ra_c$	Rigid-rigid $Ra_c$	Rigid-rigid $Ra_c$
0	1707.8	1707.83	1707.80
10	1713.0	1712.74	1712.85
100	1756.60	1756.41	1756.98
500	1940.30	1940.26	1931.03
1000	2151.70	2151.39	2116.38

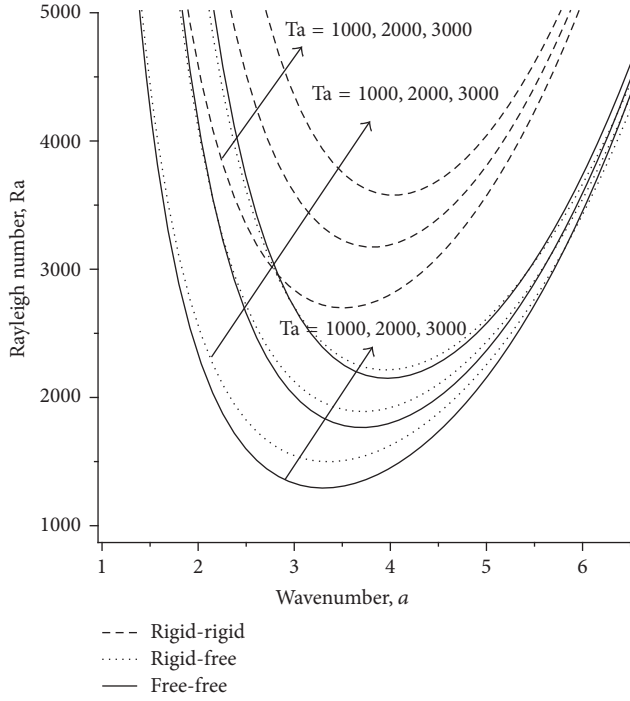


FIGURE 3: Impact of Ta on Ra against  $a$ .

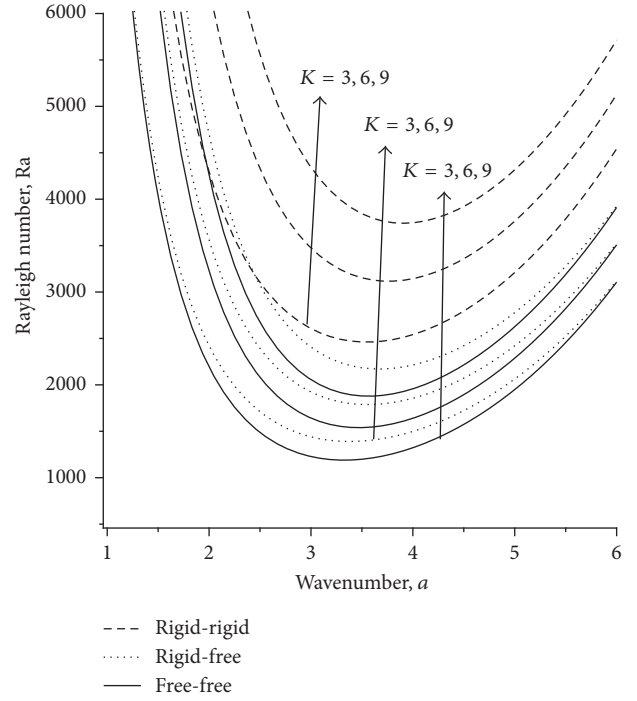


FIGURE 4: Impact of K on Ra against  $a$ .

the vorticity introduced by the rotation mechanism. Therefore, the velocity of the fluid in the vertical plane is reduced, thereby minimising the amount of thermal convection.

Figure 4 shows the response of the Rayleigh number with different values of proportional feedback control,  $K$ , on the convection instability in a nanofluid layer. From the graph, it can be seen that the values of  $Ra$  elevate proportionally as the controller  $K$  increases with all types of boundary conditions considered. This reveals that the controller is capable for delaying the onset of steady convection in a nanofluid layer. Physically, the sensors detect the departure of the fluid from its conductive state and then they direct the actuators to take action so as to suppress any disturbances [69].

The impacts of two important types of interdiffusion which are Soret ( $Sr$ ) and Dufour ( $Df$ ) parameters that arise due to the combination of temperature and concentration gradients in a nanofluid system are depicted in Figures 5 and 6, respectively. In Figure 5, the values of  $Ra$  decrease as the parameter  $Sr$  increases and thus promotes the rate of convection in the system. This occurs because of the increase

in the temperature flux, which contributes to the acceleration of the onset of convection. In contrast with the effect of  $Sr$ , and the influence of the Dufour parameter increases the Rayleigh number and stabilizes the system as can be seen in Figure 6. It is observed that this is due to the energy flux from the lower to the higher solute concentration driven by the mass gradient in the system.

The linear instability thresholds of the modified diffusivity ratio  $N_A = D_T \Delta T^* / D_B T_u^* (\phi_u^* - \phi_l^*)$  on the Rayleigh number  $Ra$  are plotted in Figure 7 for  $N_A = 2, 6$ , and  $10$ .  $Ra$  decreases slightly with an increase of  $N_A$  for three types of lower-upper boundary conditions. This phenomenon occurs because the parameter  $N_A$  is directly proportional to the thermophoretic diffusion coefficient  $D_T$ , where an increasing  $D_T$  indicates an instability in the temperature difference within the nanofluid layer. Therefore, as  $N_A$  increases the thermal instability also increases and destabilizes the system. It is interesting to note that the modified particle density,  $N_B$ , has no significant effect on the nanofluid system. An attempt has been made to scrutinize the effect of  $N_B$  in this study but

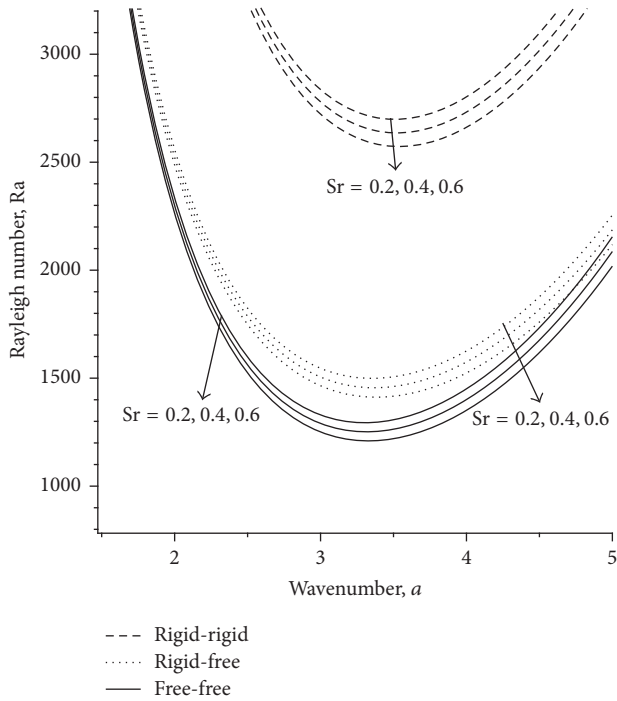


FIGURE 5: Impact of  $Sr$  on  $Ra$  against  $a$ .

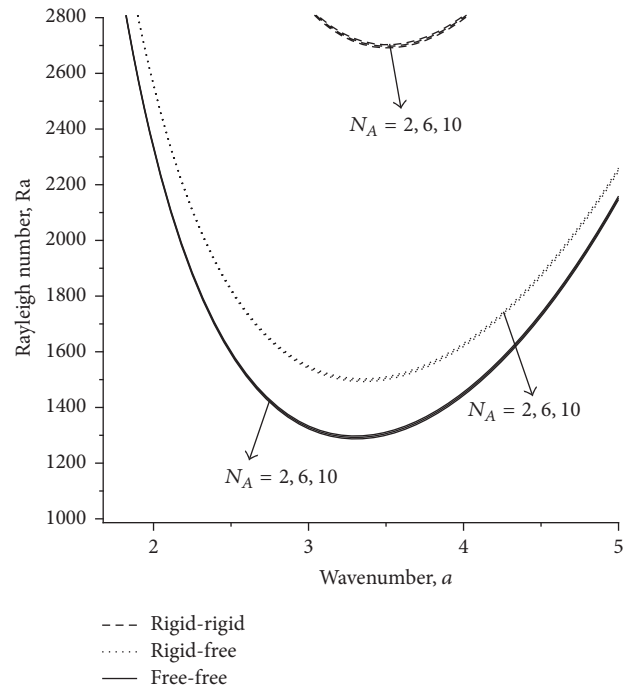


FIGURE 7: Impact of  $N_A$  on  $Ra$  against  $a$ .

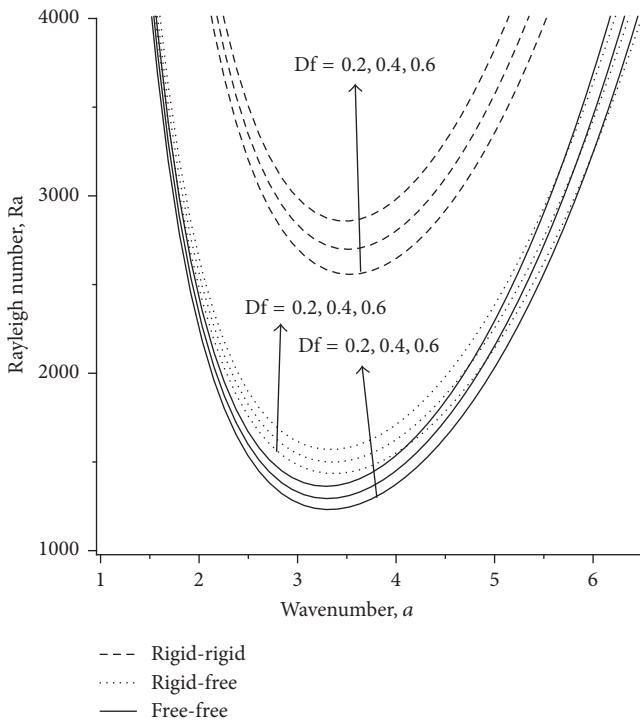


FIGURE 6: Impact of  $Df$  on  $Ra$  against  $a$ .

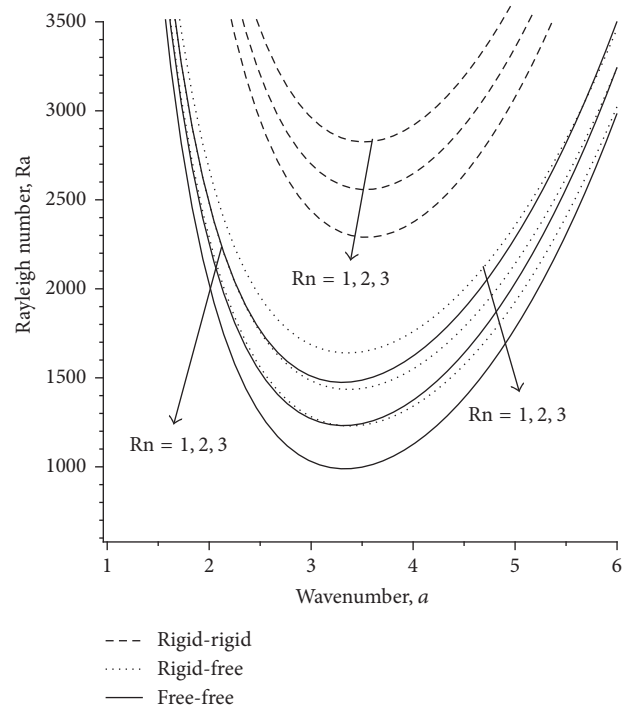


FIGURE 8: Impact of  $Rn$  on  $Ra$  against  $a$ .

there are no apparent results. This finding agrees well with those reported in [53, 54, 56] that the impact of  $N_B$  is so small that can be omitted.

Figure 8 shows the Rayleigh number  $Ra$  versus the wavenumber  $a$  for various positive values of the nanoparticle concentration Rayleigh number with various boundary

conditions. Theoretically, an increase of  $Rn$  will increase the nanoparticle volume fraction,  $\phi^*$ , because  $Rn$  is directly proportional to  $\phi^*$  according to the definition  $Rn = (\rho_p - \rho)(\phi_u^* - \phi_l^*)gL^3 / \mu\alpha_f$ . The increase of  $\phi^*$  results in a combination of Brownian motion and thermophoresis diffusion within the nanofluid layer and thus destabilizes the system. As can be

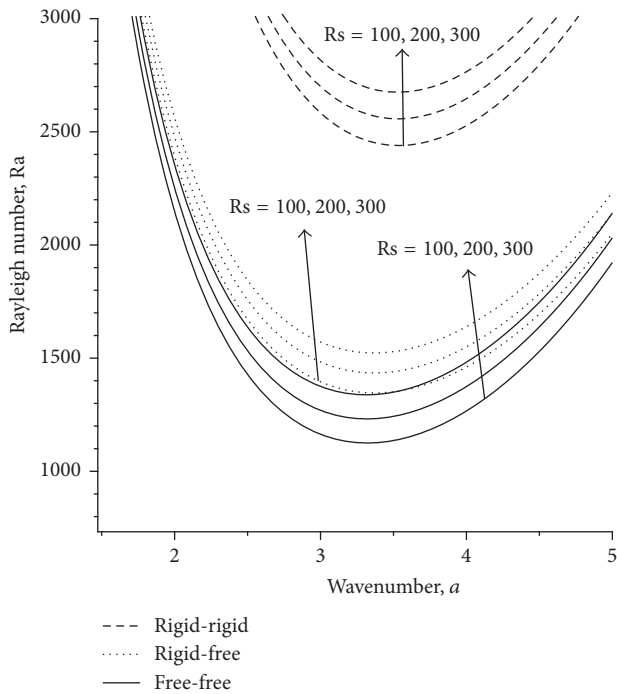


FIGURE 9: Impact of  $R_s$  on  $R_a$  against  $a$ .

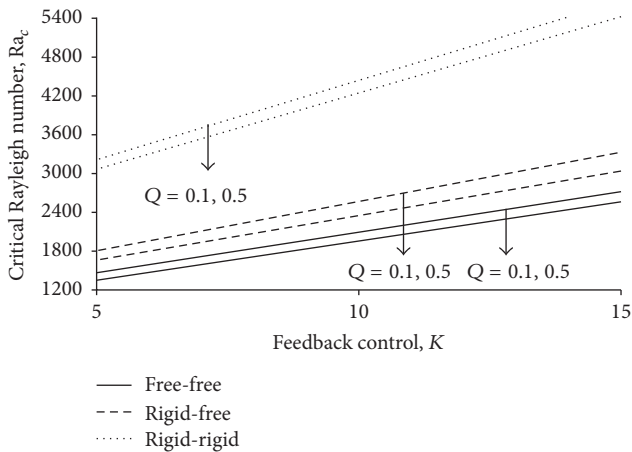


FIGURE 10: Plot of  $R_{a_c}$  with  $K$  for selected values of  $Q$ .

seen clearly in the graph, the Rayleigh number decreases as  $R_n$  increase and thus hastens the convection in the system.

The marginal stability curves for various solutal Rayleigh numbers are displayed in Figure 9 for a double-diffusive rotating nanofluid layer. The chosen values of  $R_s$  have positive and significant impact on the stability of the nanofluid layer, where it is found that  $R_a$  increases monotonically with an increase of  $R_s$ . Therefore, the onset of convection can be postponed within the nanofluid layer because the amount of solute concentration is greater than that of the solvent, leading to a decrease in the overall temperature within the system.

The graphs of critical Rayleigh number against feedback control for different values of internal heat source and Soret parameter are depicted in Figures 10 and 11, respectively. As

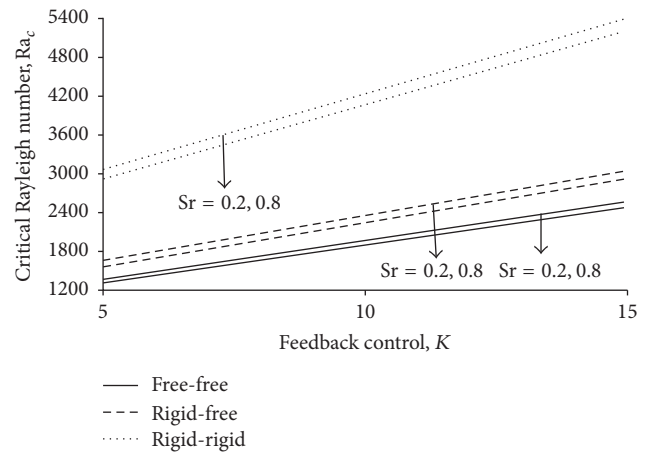


FIGURE 11: Plot of  $R_{a_c}$  with  $K$  for selected values of  $S_r$ .

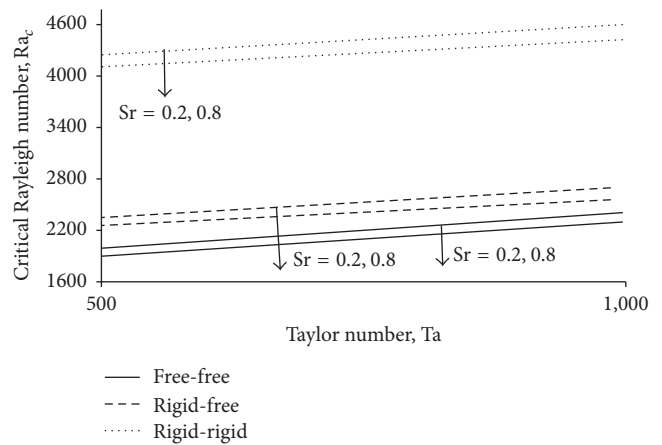


FIGURE 12: Plot of  $R_{a_c}$  with  $T_a$  for selected values of  $S_r$ .

illustrated earlier, the impact of increasing both internal heat source and Soret parameter suppressed the critical Rayleigh number monotonically. However, elevating the feedback control,  $K$ , is to delay the onset of double-diffusive convection in rotating nanofluid layer and stabilize the system.

The influences of the Taylor number,  $T_a$ , and Soret parameter are presented in Figure 12. Obviously, increasing the Coriolis force in double-diffusive nanofluid layer helps to reduce the rate of disturbance caused by  $S_r$  and thus promotes stability within the nanofluid layer. Scrutinizing the critical Rayleigh number with different boundary conditions, the rigid-rigid boundaries maintain gaining the highest values of  $R_{a_c}$  compared to the free-free and rigid-free boundaries.

The combined effects of the Dufour and Soret inter-diffusions on the critical Rayleigh number  $R_{a_c}$  are shown in Figure 13. From the graph, the stability in a horizontal nanofluid layer on the onset of double-diffusive convection is significantly altered by both effects.  $R_{a_c}$  decreases slightly with increasing of  $S_r$  for  $D_f = 0.4$  and  $0.8$ , and thus it hastens the onset of convection. Increasing the value of  $D_f$  stabilizes the system.

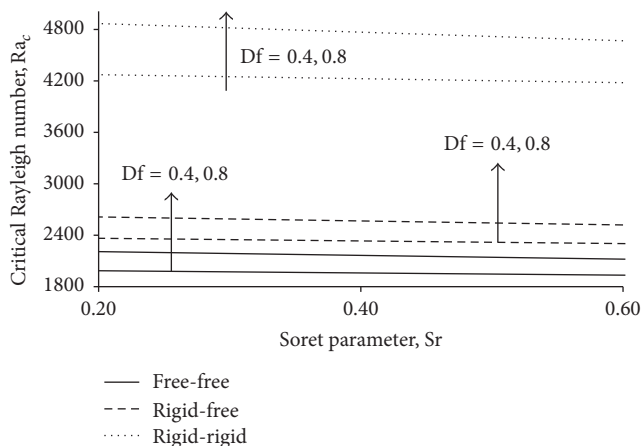


FIGURE 13: Plot of  $Ra_c$  with  $Sr$  for selected values of  $Df$ .

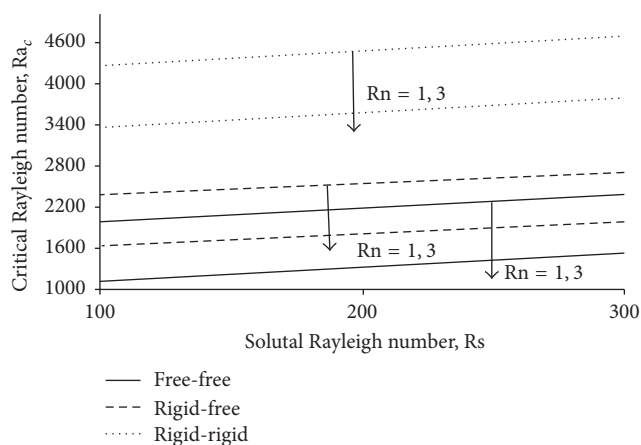


FIGURE 14: Plot of  $Ra_c$  with  $Rs$  for selected values of  $Rn$ .

Lastly, Figure 14 shows the effect of the nanoparticle concentration Rayleigh number,  $Rn$ , with various values of the solutal Rayleigh numbers,  $Rs$ .  $Rn$  always has a destabilizing effect on the system and this is in contrast to the effect of  $Rs$ , which stabilize the nanofluid layer.

#### 4. Conclusion

The effect of internal heat source on the double-diffusive convection in a rotating nanofluid layer with feedback control strategy is analyzed theoretically. Linear stability theory is applied and the eigenvalue solution is obtained numerically using the Galerkin technique. Focusing on the stationary convection, the influence of increasing the internal heat source is found to suppress the critical Rayleigh number in a nanofluid layer and thus destabilizes the system. However, the onset of convection in a double-diffusive rotating nanofluid layer can be delayed with the use of feedback control. The controller retards the loss of stability, which means helping to reduce the intensity of the Rayleigh–Bénard convection thus sustaining the stability of the system. As for the double-diffusive coefficients, an increase of the Dufour parameter

helps to slow down the destabilizing process and the opposite outcome can be seen when increasing the values of the Soret parameter, from which one can conclude that Soret parameter drives a destabilization effect within the system. It has also been seen that the influence of increasing the effect of  $Rs$  is to cause a lag in the onset of heat transfer, and an increase in  $Rn$  and  $N_A$  advances the onset of convection while the modified particle-density increment  $N_B$  has no significant impact on the system. It is worth mentioning that the critical Rayleigh number recorded for rigid-rigid horizontal boundaries is the highest and this indicates that the rigid-rigid horizontal boundaries is the most stable compared to the free-free and rigid-free horizontal boundaries.

#### Conflicts of Interest

The authors declare that there are no conflicts of interest regarding the publication of this paper.

#### Acknowledgments

The authors would like to thank the Ministry of Higher Education (MOHE) for FRGS Vote no. 5524808 and UPM Vote no. 9481900.

#### References

- [1] S. U. S. Choi, "Enhancing thermal conductivity of fluids with nanoparticles," in *Developments Applications of Non-Newtonian Flows*, D. A. Siginer and H. P. Wang, Eds., pp. 99–105, The American Society of Mechanical Engineers, Maryland, Md, USA, 1995.
- [2] H. Masuda, A. Ebata, K. Teramae, and N. Hishinuma, "Alteration of thermal conductivity and viscosity of liquid by dispersing ultra-fine particles," *Netsu Bussei*, vol. 7, no. 4, pp. 227–233, 1993.
- [3] Y. Xuan and Q. Li, "Heat transfer enhancement of nanofluids," *International Journal of Heat and Fluid Flow*, vol. 21, no. 1, pp. 58–64, 2000.
- [4] J. A. Eastman, S. U. S. Choi, S. Li, W. Yu, and L. J. Thompson, "Anomalous increased effective thermal conductivities of ethylene glycol-based nanofluids containing copper nanoparticles," *Applied Physics Letters*, vol. 78, no. 6, pp. 718–720, 2001.
- [5] S. K. Das, N. Putra, P. Thiesen, and W. Roetzel, "Temperature dependence of thermal conductivity enhancement for nanofluids," *Journal of Heat Transfer*, vol. 125, no. 4, pp. 567–574, 2003.
- [6] J. Buongiorno, "Convective transport in nanofluids," *Journal of Heat Transfer*, vol. 128, no. 3, pp. 240–250, 2006.
- [7] D. Y. Tzou, "Instability of nanofluids in natural convection," *ASME Journal of Heat Transfer*, vol. 130, no. 7, Article ID 072401, 9 pages, 2008.
- [8] D. Y. Tzou, "Thermal instability of nanofluids in natural convection," *International Journal of Heat and Mass Transfer*, vol. 51, no. 11-12, pp. 2967–2979, 2008.
- [9] Z. Alloui, P. Vasseur, and M. Reggio, "Natural convection of nanofluids in a shallow cavity heated from below," *International Journal of Thermal Sciences*, vol. 50, no. 3, pp. 385–393, 2011.
- [10] D. A. Nield and A. V. Kuznetsov, "The onset of convection in a horizontal nanofluid layer of finite depth," *European Journal of Mechanics. B. Fluids*, vol. 29, no. 3, pp. 217–223, 2010.

- [11] D. Yadav, G. S. Agrawal, and R. Bhargava, "Rayleigh-Bénard convection in nanofluid," *International Journal of Applied Mathematics and Mechanics*, vol. 7, pp. 61–76, 2011.
- [12] Z. Haddad, E. Abu-Nada, H. F. Oztop, and A. Mataoui, "Natural convection in nanofluids: are the thermophoresis and Brownian motion effects significant in nanofluid heat transfer enhancement?" *International Journal of Thermal Sciences*, vol. 57, pp. 152–162, 2012.
- [13] U. Gupta, J. Sharma, and R. K. Wanchoo, "Thermosolutal convection in a horizontal nanofluid layer: introduction of oscillatory motions," in *Proceedings of the Recent Advances in Engineering and Computational Sciences (RAECS '14)*, pp. 1–6, IEEE, Chandigarh, India, March 2014.
- [14] M. S. Ayano, "Mixed convection flow micropolar fluid over a vertical plate subject to hall and ionslip currents," in *Proceedings of the Mixed convection flow micropolar fluid over a vertical plate subject to hall and ion-slip currents*, vol. 5, pp. 38–52, 2013.
- [15] D. T. J. Hurle and E. Jakeman, "Soret-driven thermosolutal convection," *Journal of Fluid Mechanics*, vol. 47, no. 4, pp. 667–687, 1971.
- [16] J. K. Platten and G. Chavepeyer, "Oscillatory motion in Bénard cell due to the Soret effect," *Journal of Fluid Mechanics*, vol. 60, no. 2, pp. 305–319, 1973.
- [17] D. R. Caldwell, "Non-linear effects in a Rayleigh-Bénard experiment," *Journal of Fluid Mechanics*, vol. 42, no. 1, pp. 161–175, 1970.
- [18] E. Knobloch and D. R. Moore, "Linear stability of experimental Soret convection," *Physical Review A*, vol. 37, no. 3, pp. 860–870, 1988.
- [19] A. Bergeon, D. Henry, H. Benhadid, and L. S. Tuckerman, "Marangoni convection in binary mixtures with Soret effect," *Journal of Fluid Mechanics*, vol. 375, pp. 143–177, 1998.
- [20] S. Slavtchev, G. Simeonov, S. Van Vaerenbergh, and J. C. Legros, "Marangoni instability of a layer of binary liquid in the presence of nonlinear Soret effect," *International Journal of Heat and Mass Transfer*, vol. 42, no. 15, pp. 3007–3011, 1999.
- [21] S. Saravanan and T. Sivakumar, "Exact solution of Marangoni convection in a binary fluid with throughflow and Soret effect," *Applied Mathematical Modelling. Simulation and Computation for Engineering and Environmental Systems*, vol. 33, no. 9, pp. 3674–3681, 2009.
- [22] D. A. Nield and A. V. Kuznetsov, "The onset of double-diffusive convection in a nanofluid layer," *International Journal of Heat and Fluid Flow*, vol. 32, no. 4, pp. 771–776, 2011.
- [23] A. V. Kuznetsov and D. A. Nield, "The onset of double-diffusive nanofluid convection in a layer of a saturated porous medium," *Transport in Porous Media*, vol. 85, no. 3, pp. 941–951, 2010.
- [24] D. Yadav, G. S. Agrawal, and R. Bhargava, "The onset of convection in a binary nanofluid saturated porous layer," *International Journal of Theoretical and Applied Multiscale Mechanics*, vol. 2, no. 3, pp. 198–224, 2012.
- [25] D. Yadav, G. S. Agrawal, and R. Bhargava, "Onset of double-diffusive nanofluid convection in a layer of saturated porous medium with thermal conductivity and viscosity variation," *Journal of Porous Media*, vol. 16, no. 2, pp. 105–121, 2013.
- [26] S. Agarwal, N. C. Sacheti, P. Chandran, B. S. Bhadauria, and A. K. Singh, "Non-linear convective transport in a binary nanofluid saturated porous layer," *Transport in Porous Media*, vol. 93, no. 1, pp. 29–49, 2012.
- [27] R. Chand and G. C. Rana, "Magneto convection in a layer of nanofluid with soret effect," *Acta Mechanica et Automatica*, vol. 9, no. 2, 2015.
- [28] N. Akbar, Z. Khan, S. Nadeem, and W. Khan, "Double-diffusive natural convective boundary-layer flow of a nanofluid over a stretching sheet with magnetic field," *International Journal of Numerical Methods for Heat & Fluid Flow*, vol. 26, no. 1, pp. 108–121, 2016.
- [29] S. N. Gaikwad and S. S. Kamble, "Cross-diffusion effects on the onset of double diffusive convection in a couple stress fluid saturated rotating anisotropic porous layer," *Journal of Applied Fluid Mechanics*, vol. 9, no. 4, pp. 1645–1654, 2016.
- [30] S. P. Bhattacharyya and S. K. Jena, "Thermal instability of a horizontal layer of micropolar fluid with heat source," *Indian Academy of Sciences. Proceedings. Mathematical Sciences*, vol. 93, no. 1, pp. 13–26, 1984.
- [31] M.-I. Char and K.-T. Chiang, "Stability analysis of Bénard-Marangoni convection in fluids with internal heat generation," *Journal of Physics D: Applied Physics*, vol. 27, no. 4, pp. 748–755, 1994.
- [32] N. F. M. Mokhtar, N. M. Arifin, R. Nazar, F. Ismail, and M. Suleiman, "Marangoni convection in a liquid saturated porous medium with interval heat generation," *Far East Journal of Applied Mathematics*, vol. 34, no. 2, pp. 269–283, 2009.
- [33] N. F. M. Mokhtar, N. M. Arifin, R. Nazar, F. Ismail, and M. Suleiman, "Effect of internal heat generation on Marangoni convection in a fluid saturated porous medium," *International Journal of Applied Mathematics and Statistics*, vol. 19, pp. 112–122, 2010.
- [34] N. F. M. Mokhtar, N. M. Arifin, R. Nazar, F. Ismail, and M. Suleiman, "Effect of internal heat generation on Marangoni convection in a superposed fluid-porous layer with deformable free surface," *International Journal of Physical Sciences*, vol. 6, no. 23, pp. 5550–5563, 2011.
- [35] F. Capone, M. Gentile, and A. A. Hill, "Double-diffusive penetrative convection simulated via internal heating in an anisotropic porous layer with throughflow," *International Journal of Heat and Mass Transfer*, vol. 54, no. 7-8, pp. 1622–1626, 2011.
- [36] B. S. Bhadauria, A. Kumar, J. Kumar, N. C. Sacheti, and P. Chandran, "Natural convection in a rotating anisotropic porous layer with internal heat generation," *Transport in Porous Media*, vol. 90, no. 2, pp. 687–705, 2011.
- [37] N. F. M. Mokhtar, I. K. Khalid, and N. M. Arifin, "Effect of internal heat generation on benard-marangoni convection in micropolar fluid with feedback control," *Journal of Physics: Conference Series*, vol. 435, no. 1, Article ID 012029, 2013.
- [38] I. K. Khalid, N. F. M. Mokhtar, and N. M. Arifin, "Uniform solution on the combined effect of magnetic field and internal heat generation on rayleigh-Bénard convection in micropolar fluid," *Journal of Heat Transfer*, vol. 135, no. 10, Article ID 102502, 2013.
- [39] D. Yadav, R. Bhargava, and G. S. Agrawal, "Boundary and internal heat source effects on the onset of Darcy-Brinkman convection in a porous layer saturated by nanofluid," *International Journal of Thermal Sciences*, vol. 60, pp. 244–254, 2012.
- [40] D. Yadav, C. Kim, J. Lee, and H. H. Cho, "Influence of magnetic field on the onset of nanofluid convection induced by purely internal heating," *Computers & Fluids*, vol. 121, pp. 26–36, 2015.
- [41] D. A. Nield and A. V. Kuznetsov, "The onset of convection in an internally heated nanofluid layer," *Journal of Heat Transfer*, vol. 136, no. 1, Article ID 014501, 2014.
- [42] A. Wakif, Z. Boualahia, and R. Sehaqui, "Numerical study of a thermal convection induced by a purely internal heating

- in a rotating medium saturated by a radiating nanofluid," *International Journal of Computer Applications*, vol. 135, no. 10, pp. 33–42, 2016.
- [43] S. Chandrasekhar, *Hydrodynamic and Hydromagnetic stability*, Oxford University Press, Oxford, UK, 1961.
- [44] A. Vidal and A. Acrivos, "The influence of Coriolis force on surface-tension-driven convection," *Journal of Fluid Mechanics*, vol. 26, no. 4, pp. 807–818, 1966.
- [45] G. A. McConaghy and B. A. Finlayson, "Surface tension driven oscillatory instability in a rotating fluid layer," *Journal of Fluid Mechanics*, vol. 39, no. 1, pp. 49–55, 1969.
- [46] M. Takashima and T. Namikawa, "Surface-tension-driven convection under the simultaneous action of a magnetic field and rotation," *Physics Letters A*, vol. 37, no. 1, pp. 55–56, 1971.
- [47] R. Friedrich and N. Rudraiah, "Marangoni convection in a rotating fluid layer with non-uniform temperature gradient," *International Journal of Heat and Mass Transfer*, vol. 27, no. 3, pp. 443–449, 1984.
- [48] A. Douiebe, M. Hannaoui, G. Lebon, A. Benaboud, and A. Khmou, "Effects of a.c. electric field and rotation on Bénard-Marangoni convection," *Flow, Turbulence and Combustion*, vol. 67, no. 3, pp. 185–204, 2001.
- [49] T. Namikawa, M. Takashima, and S. Matsushita, "The effect of rotation on convective instability induced by surface tension and buoyancy," *Journal of the Physical Society of Japan*, vol. 28, no. 5, pp. 1340–1349, 1970.
- [50] A. Kaddame and G. Lebon, "Bénard-Marangoni convection in a rotating fluid with and without surface deformation," *Applied Scientific Research*, vol. 52, no. 4, pp. 295–308, 1994.
- [51] A. Kaddame and G. Lebon, "Overstability in rotating Bénard-Marangoni cells," in *Microgravity Quart*, pp. 69–74, 1994.
- [52] I. Hashim and W. Sarma, "The effect of Coriolis force on Marangoni convection," in *Proceedings of the 15th Australasian Fluid Mechanics Conference*, 2004.
- [53] D. Yadav, G. S. Agrawal, and R. Bhargava, "Thermal instability of rotating nanofluid layer," *International Journal of Engineering Science*, vol. 49, no. 11, pp. 1171–1184, 2011.
- [54] D. Yadav, R. Bhargava, and G. S. Agrawal, "Numerical solution of a thermal instability problem in a rotating nanofluid layer," *International Journal of Heat and Mass Transfer*, vol. 63, pp. 313–322, 2013.
- [55] D. Yadav, R. Bhargava, G. S. Agrawal, G. S. Hwang, J. Lee, and M. C. Kim, "Magneto-convection in a rotating layer of nanofluid," *Asia-Pacific Journal of Chemical Engineering*, vol. 9, no. 5, pp. 663–677, 2014.
- [56] D. Yadav, G. S. Agrawal, and J. Lee, "Thermal instability in a rotating nanofluid layer: a revised model," *Ain Shams Engineering Journal*, vol. 7, no. 1, pp. 431–440, 2016.
- [57] Y. Z. Wang, J. Singer, and H. H. Bau, "Controlling chaos in a thermal convection loop," *Journal of Fluid Mechanics*, vol. 237, pp. 479–498, 1992.
- [58] J. Tang, *Active control of Rayleigh-Bénard convection [Ph.D. thesis]*, University of Pennsylvania, 1996.
- [59] J. Tang and H. H. Bau, "Stabilization of the no-motion state in Rayleigh-Bénard convection through the use of feedback control," *Physical Review Letters*, vol. 70, no. 12, pp. 1795–1798, 1993.
- [60] J. Tang and H. H. Bau, "Feedback control stabilization of the no-motion state of a fluid confined in a horizontal porous layer heated from below," *Journal of Fluid Mechanics*, vol. 257, pp. 485–505, 1993.
- [61] J. Tang and H. H. Bau, "Stabilization of the no-motion state in the Rayleigh-Bénard problem," *Proceedings of the Royal Society of London A*, vol. 447, pp. 587–607, 1994.
- [62] J. Tang and H. H. Bau, "Stabilization of the no-motion state of a horizontal fluid layer heated from below with Joule heating," *Journal of Heat Transfer*, vol. 117, no. 2, pp. 329–333, 1995.
- [63] J. Tang and H. H. Bau, "Experiments on the stabilization of the no-motion state of a fluid layer heated from below and cooled from above," *Journal of Fluid Mechanics*, vol. 363, pp. 153–171, 1998.
- [64] J. Tang and H. H. Bau, "Numerical investigation of the stabilization of the no-motion state of a fluid layer heated from below and cooled from above," *Physics of Fluids*, vol. 10, no. 7, pp. 1597–1610, 1998.
- [65] L. E. Howle, "Control of Rayleigh-Bénard convection in a small aspect ratio container," *International Journal of Heat and Mass Transfer*, vol. 40, no. 4, pp. 817–822, 1997.
- [66] L. E. Howle, "Active control of Rayleigh-Bénard convection," *Physics of Fluids*, vol. 9, no. 7, pp. 1861–1863, 1997.
- [67] L. E. Howle, "Linear stability analysis of controlled Rayleigh-Bénard convection using shadowgraphic measurement," *Physics of Fluids*, vol. 9, no. 11, pp. 3111–3113, 1997.
- [68] H. Hu and H. H. Bau, "Feedback control to delay or advance liner loss of stability in planar Poiseuille flow," *A*, vol. 447, pp. 299–312, 1994.
- [69] H. H. Bau, "Control of Marangoni-Bénard convection," *International Journal of Heat and Mass Transfer*, vol. 42, no. 7, pp. 1327–1341, 1999.
- [70] N. Bachok, N. M. Arifin, and F. M. Ali, "Effects of control on the onset of Marangoni-Bénard convection with uniform internal heat generation," *International Journal of Mathematics and Computer Science*, vol. 24, pp. 23–29, 2008.
- [71] I. Hashim and Z. Siri, "Stabilization of steady and oscillatory marangoni instability in rotating fluid layer by feedback control strategy," *Numerical Heat Transfer; Part A: Applications*, vol. 54, no. 6, pp. 647–663, 2008.
- [72] Z. Siri and I. Hashim, "Control of oscillatory of Bénard-Marangoni convection in rotating fluid layer," in *Proceedings of the 2009 International Conference on Signal Processing Systems (ICSPS '09)*, pp. 938–941, Singapore, May 2009.
- [73] Z. Siri, Z. Mustafa, and I. Hashim, "Effects of rotation and feedback control on Bénard-Marangoni convection," *International Journal of Heat and Mass Transfer*, vol. 52, no. 25–26, pp. 5770–5775, 2009.
- [74] N. H. Z. Abidin, N. F. M. Mokhtar, N. Arbin, J. M. Said, and N. M. Arifin, "Marangoni convection in a micropolar fluid with feedback control," in *Proceedings of the IEEE Symposium on Business, Engineering and Industrial Applications (ISBELA '12)*, pp. 558–562, September 2012.
- [75] I. K. Khalid, N. F. M. Mokhtar, and N. M. Arifin, "Rayleigh-Bénard convection in micropolar fluid with feedback control effect," *World Applied Sciences Journal*, vol. 21, no. 3, pp. 112–118, 2013.
- [76] BCS and Inc., "Waste heat recovery: technology and opportunities in U.S. industry," Tech. Rep., U.S. Department of Energy, Industrial Technologies Program, 2008.



# Hindawi

Submit your manuscripts at  
<https://www.hindawi.com>

